JOURNAL OF APPLIED ELECTROCHEMISTRY 25 (1995) 809–816

Cathodic process and cyclic redox reactions in aluminium electrolysis cells

Å. STERTEN

Department of Electrochemistry, The Norwegian Institute of Technology (NTH), The University of Trondheim, N-7034 Trondheim, Norway

P. A. SOLLI

Hydro Aluminium, Technology Centre Årdal, P.O. Box 303, N-5870 Øvre Årdal, Norway

Received 25 October 1994; revised 16 January 1995

The cathode processes in aluminium electrolysis cells are discussed, with detailed descriptions of the chemical reactions and transport processes leading to loss of current efficiency with respect to aluminium. The cathode current consuming reactions can be described by (i) the aluminium formation reaction, and (ii) reduction reactions forming so-called dissolved metal species (reduced entities). The rate determining steps for the aluminium forming process are mass transport of AlF_3 to the metal surface, and mass transport of NaF away from the metal surface. In commercial cells there is continuous feed of impurity species to the electrolyte, depressing the concentration of dissolved metal species to very low equilibrium values in the bulk phase of the electrolyte. However, the equilibrium values of reduced entities in the electrolyte at the metal surface are much higher than in the bulk phase. This means that polyvalent impurity species are involved in cyclic redox reactions in the electrode and gas boundary layers. The most important rate-determining steps related to these cyclic processes are (i) mass transport of reduced entities from the metal surface to a reaction plane within the cathode boundary layer, and (ii) mass transport of impurity species from the electrolyte bulk phase to the reaction plane in the cathode boundary layer. This means that there is negligible transport of dissolved metal species through the bulk of the electrolyte phase during normal operation of commercial cells.

1. Introduction

Industrial production of aluminium is now exclusively based on the Hall-Heroult process. The process involves electrochemical decomposition of alumina (Al_2O_3) dissolved in molten cryolite (Na_3AlF_6) containing some additives (AlF_3, CaF_2, MgF_2 and/or LiF). The consumable carbon anode liberates CO_2 with a current efficiency close to 100% [1], while the cathodic current efficiency (CE) with respect to aluminium normally ranges from 87 to 96% in commercial cells. The main overall cell reaction may be written,

$$Al_2O_3 + 3/2C = 2Al + 3/2CO_2 \quad (1)$$

Considerable improvements in CE have been achieved during the last decades [2, 3], through magnetic compensation, improved cell design, improved bath chemistry including point feeding of alumina and automated cell control.

Traditionally, loss of metal or loss of current has been referred to in terms of the 'back reaction',

$$2\langle Al\rangle + 3CO_2 = Al_2O_3 + 3CO \quad (2)$$

where $\langle Al\rangle$ is dissolved aluminium in the form of reduced entities produced on the metal surface. At high current efficiencies the amount of CO formed roughly corresponds to the loss in cathodic current efficiency [4]. However, an analysis of the process taking place in commercial cells [5, 6], has revealed that polyvalent impurities are involved in cyclic redox reactions taking place in the electrolyte/metal and the electrolyte/anode gas boundary layers. The process is composed of several reactions and transport steps, which means that any reaction site for Reaction 2 cannot be localized during normal cell operations. Instead of using the term 'back reaction' we will refer to the process leading to current inefficiency as the 'loss process'. Most of the work done on the mechanism of the cathode process supports the idea of interlinked mass transfer processes of several entities in the cathodic boundary layer being the most important rate determining steps, both for the aluminium deposition reaction and for the loss process [7, 8].

The present work is a review leading to a new and detailed description of the cathode process, including cyclic redox reactions and transport processes, both in laboratory and commercial aluminium electrolysis cells. Rate limiting steps both for the aluminium deposition reaction and for the loss process are discussed in view of theoretical considerations and

0021-891X

literature data. However, the kinetics of the aluminium deposition reaction will not be discussed in the present context since the reaction proceeds with a very high exchange current density [8] and is thus not involved in any rate limiting steps. Other loss processes like codeposition of impurities, carbide formation, physical short-circuiting and losses due to dispersion of aluminium under extreme convective conditions are discussed briefly. The present work will serve as a necessary background for deriving a CE model to be described in a future presentation.

For several years we have been working with models related to current efficiency in aluminium electrolysis cells. Considerable effort has been put into the design and development of a laboratory cell for the study of CE as a function of melt composition, temperature and current density. The quantitative influence of impurities on CE and the mechanistic role impurities play in the loss process have also been studied. The present paper, partly emerging from this work, is the first in a series of papers to be published in this field.

2. Cathode process including the loss process

It is well known that aluminium reacts with cryolite melts through formation of reduced entities soluble in the electrolyte. The rate of the loss process is defined as the rate of transport of these species away from the cathode surface. There is an obvious need for a detailed understanding of the structure of these entities including transport properties and concentration/activity relationships.

There have been numerous laboratory studies on the rate of aluminium loss and the rate of reaction between dissolved metal and CO_2. Grjotheim *et al.* [8] have reviewed some of these results, and conclude that mass transfer at the melt/metal interface is the most probable rate determining step for the process of metal/current loss. Some influence of mass transport at the melt/gas interface cannot, according to Grjotheim *et al.*, be completely ruled out. The rate of mass transport in the bulk phase in commercial cells is much higher than the rate of mass transport in the boundary layers, and should not be considered as a rate limiting step. This means that in the following discussion the electrolyte will be considered to be of homogeneous composition.

2.1. *Nature of dissolved metal*

Several research groups have studied the reduced entities formed when aluminium reacts with cryolitic melts, but still the nature and concentrations of the most probable reduced entities formed at the aluminium surface are controversial. There appears to be general agreement [8] that the equilibrium,

$$Al + 3NaF = AlF_3 + 3Na \qquad (3)$$

is rapidly established at the electrolyte/metal interface. The equilibrium concentration of dissolved Na in the salt phase increases with increasing NaF/AlF_3 ratio. In addition subvalent aluminium species are formed, the ionic structures of which are discussed below. It should be emphasized that the equilibrium concentration of dissolved neutral Al atoms in the liquid electrolyte phase is expected to be extremely low.

The total solubility or the amount of aluminium reacted with the melt, was found to increase with increasing NaF/AlF_3 ratio [9–12]. The most accurate data on total amount of aluminium reacted are those of Ødegård *et al.* [11], who determined the equilibrium content by a careful quenching technique. Several ionic models were fitted to the total solubility data as a function of NaF/AlF_3 ratio. The final result indicated that the most important reduced entities at intermediate NaF/AlF_3 ratios were Na and AlF_2^-. At low NaF/AlF_3 ratios some additional species should be present, and entities like $Al_2F_3^-$, $Al_3F_4^-$ and $Al_4F_5^-$ were suggested. The species AlF, Al^+, Al^{2+} and Na_2^+ were ruled out as significant entities in melts of commercial interest [11].

Diffusion coefficients for ionic species in molten salts are usually in the order of $10^{-5}\,cm^2\,s^{-1}$, while the estimated diffusivity based on the total amount of aluminium reacted appear to be considerably higher, as found by Dewing and Yoshida [13], Borisoglebskii *et al.* [14] and Ødegård [15]. The results indicate the presence of sodium with some kind of electronic nature. Bredig [16] demonstrated electronic conduction in alkali metal-alkali metal salt mixtures, such as the Na–NaF system. The Na–NaF system is a part of the system Al–NaF–AlF_3–Al_2O_3 due to formation of sodium on the aluminium surface, Reaction 3. Electronic conduction may, therefore, play an important role in the loss process. The true nature of dissolved sodium/electrons is not fully understood, although Egan and Freyland [17], Haarberg *et al.* [18] and Lui and Poignet [19] have shown that sodium–sodium halide systems can formally be described in terms of defect equilibria involving concentrations or activities of various types of trapped electrons, comparable with F-centres in the solid state, and electrons excited into weak localized states of the conduction band of the electrolyte. Electrons in the conduction band are expected to have a higher diffusivity than trapped electrons. From [17–19] it must be expected that there is some proportionality between the equilibrium activity of sodium and the concentration of electrons in sodium–sodium halide systems. There does not, however, appear to be sufficient data available to accurately model the concentration of electrons as a function of sodium activity in the Al(Na)–NaF–AlF_3 based systems. Haarberg *et al.* [20] determined the electronic contribution to total conductivity in the Na_3AlF_6(l)–Al_2O_3(s)–Na(Bi)(l) system as a function of sodium activity in the Na–Bi alloy. They calculated the diffusion coefficient of electrons to be approximately $0.03\,cm^3\,s^{-1}$, i.e. roughly three orders of magnitude higher than

normal ionic diffusivities, indicating that electronic conduction is important in the loss process.

Dewing [21] proposed that the solubility data of Ødegård *et al.* [11] could be explained by a degenerate electron gas model. These electrons located in a conduction band, apparently explained the total solubility from pure NaF down to a NaF/AlF_3 molar ratio of 1.25. However, the proposed hypothesis including the fit to experimental data are based on assumptions which are not easily verified.

From the above discussion it follows that there is some uncertainty as to the nature of the species formed, when Al reacts with the melt. We still believe that Na and AlF_2^- are the main species, and that dissolved Na possesses electronic properties. The formation of these species can be viewed as a classical corrosion process as described by the following heterogenous redox reactions: Anodic dissolution of Al,

$$Al + 3NaF = AlF_3 + 3Na^+ + 3e^- \quad (4)$$

and cathodic formation of reduced entities,

$$Na^+ + e^- = Na \quad (5)$$

$$1/2Na^+ + 1/2AlF_3 + e^- = 1/2AlF_2^- + 1/2NaF \quad (6)$$

The equilibrium concentration of electrons (trapped and/or in the conduction band), somehow related to the concentration or the activity of dissolved sodium, cannot be evaluated without a structure model. However, the overall electrode side reaction may tentatively be written,

$$e^- = e' \quad (7)$$

where e' denotes an electron in an unspecified state in the cathode boundary layer of the electrolyte phase.

2.2. *Main cathode reaction: Concentration gradients and rate limiting steps*

The primary overall cathode reaction is preferably written in the following way,

$$AlF_3 + 3Na^+ + 3e^- = Al + 3NaF \quad (8)$$

The process can be divided into two steps: (i) mass transport of AlF_3 through the cathode boundary layer and a corresponding transport of NaF in the opposite direction; and (ii) the overall charge transfer Reaction 8. Experimental data from Piontelli *et al.* [22, 23], Thonstad and Rolseth [24, 25] and Sum and Skyllas Kazacos [26] show that the cathode process, including side reactions, proceeds with *low* charge transfer overvoltage, and that cathodic overvoltage can be roughly treated as concentration overvoltage. Slow diffusion gives rise to concentration gradients in the cathode boundary layer.

The transference number of the sodium ion in cryolitic melts of industrial importance is close to unity [28]. The fact that sodium ions carry the current while aluminium is deposited, gives rise to increasingly steeper concentration gradients in the diffusion layer with an increase in cathodic current density. Zero applied current means that there is no net deposition of aluminium. On the contrary, corrosion reactions involving anodic dissolution of aluminium and cathodic formation of reduced entities soluble in the electrolyte take place according to the redox Reactions 4 to 7. The steady state rate of formation of reduced entities (RE) in an open system according to these reactions, results in a continuous loss of metal, and a slightly more acidic (AlF_3 rich) electrolyte composition at the electrolyte/metal interface than in the bulk phase, as indicated in

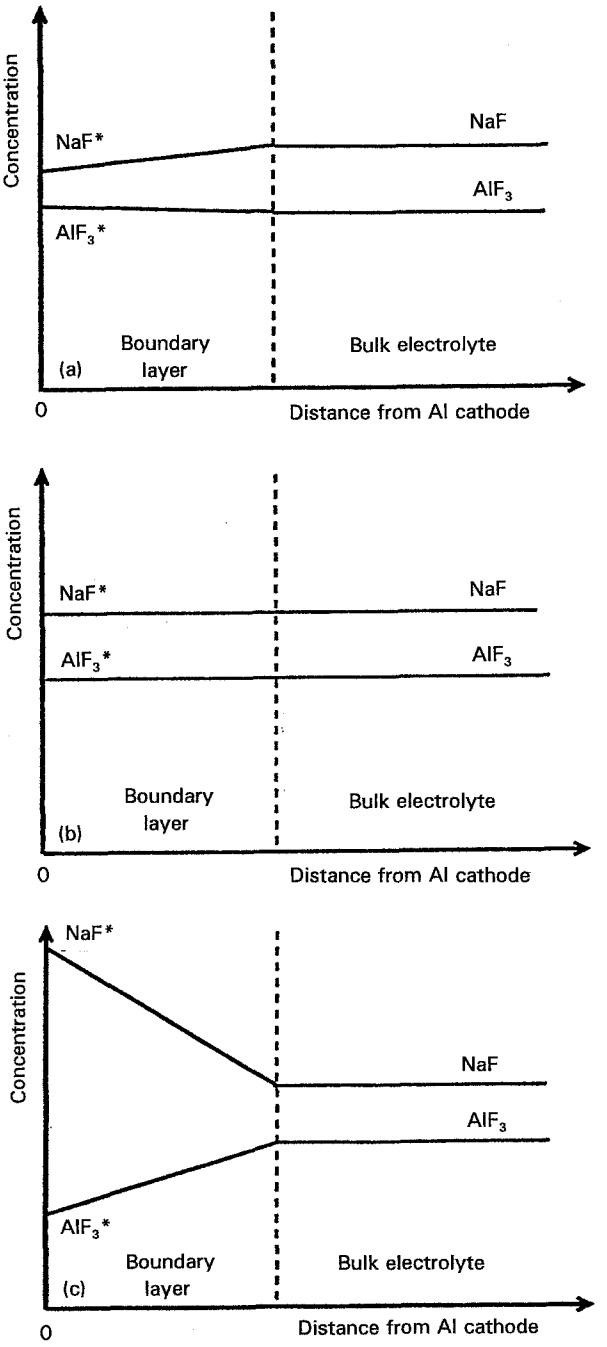

Fig. 1. Schematic concentration gradients of NaF and AlF_3 in the cathode boundary layer when (a) no external current is applied, (b) a small cathodic current is applied, and (c) a high cathodic current is applied.

Fig. 1(a). A slight increase in the externally applied current from zero, causes the rate of the anodic corrosion Reaction 4 to decrease, while the rates of the cathodic Reactions 5 to 7 increase slightly. For a small cathodic current the profile shown in Fig. 1(b) occurs (i.e., no gradients of NaF and AlF_3). Such a profile corresponds roughly to no net production or loss of aluminium. A further increase in cathodic current gives a net production of aluminium, which means that the corrosion Reaction 4 is forced to proceed in the opposite direction, Reaction 8, giving rise to the concentration profile indicated in Fig. 1(c). In this case the bath composition at the interface will be less acidic than the bulk composition. A consequence of the discussion above is that the cathodic current density must be an important parameter for the CE.

The shift in bath composition over the cathode boundary layer for a given current density can, according to Reaction 8, be related to the concentration overvoltage, η, by,

$$\eta_{Al} = \frac{RT}{F}\ln\frac{a_{NaF}}{a^*_{NaF}} + \frac{RT}{3F}\ln\frac{a^*_{AlF_3}}{a_{AlF_3}} \qquad (9)$$

where * refers to activities on the aluminium surface. From the above discussion it follows that mass transport of AlF_3 to the metal surface, and of NaF in the opposite direction, constitute the rate limiting steps for the main cathode reaction.

2.3. *Current loss and rate limiting steps*

The traditional understanding of the loss process based on an initial deposition of aluminium at 100% CE is rather unlikely, and is not a good starting point for a discussion of the loss process. As discussed above the cathodic side Reactions 5 to 7 take place even at zero external current and must be expected to slightly increase in rate when an external cathodic current is applied due to the shift in the NaF and AlF_3 concentration gradients in the boundary layer. From the above discussion it also follows that both chemical and electrochemical reactions proceed roughly at equilibrium on the metal surface, at least for current densities up to about $1\,A\,cm^{-2}$. It is convenient to separate the following discussion of the loss process into two steps: first, mass transport in the absence of electrolyte impurities, and second, mass transport in the presence of electrolyte impurities.

2.3.1. Transport processes and reactions in the absence of impurities. It is presupposed that the convective forces in the bulk of the electrolyte are so high that there will be no gradients of RE (AlF_2^-, Na or e′) in the bulk phase of the electrolyte. Then, steady state concentration gradients are established with respect to RE in the boundary layers. The individual gradients are interlinked by internal homogeneous equilibria between the various types of reduced entities, as described elsewhere [6, 7]. In the following discussion concentration gradients of RE are somewhat arbitrarily represented by the gradient of electrons (e′), which is proposed to be a unique function of the activity of sodium in agreement with previous studies [17–19]. Figure 2 shows schematic concentration gradients of electrons in the absence of impurities. By impurities are meant ions/species which can readily react with RE. At plane B (Fig. 2), somewhere in the diffusion layer towards the CO_2 gas phase, RE reacts with dissolved carbon dioxide, e.g.,

$$e' + 1/2CO_2 = 1/2O^{2-} + 1/2CO \qquad (10)$$

where O^{2-} denotes complex oxide species [29].

The overall anode reaction corresponding to the cathode side reactions 5 to 7 may be written

$$1/2O^{2-} + 1/4C = 1/4CO_2 + e^- \qquad (11)$$

Combination of one arbitrary reaction sequence 7, 10 and 11 gives the 'main overall loss process',

$$1/4CO_2 + 1/4C = 1/2CO \qquad (12)$$

which is discussed below.

The reaction scheme above is in agreement with the presently most usual way of expressing the 'back reaction', in the sense that RE are considered to be transported all the way to the gas/electrolyte interface before reacting with the anode products. However, it should be emphasized that the overall loss process must correspond to Equation 12.

Formation of carbon dust may also take place to a minor degree,

$$2e' + CO = O^{2-} + C(s) \qquad (13)$$

Some carbon dust was in fact observed by Thonstad [30], when bubbling CO_2 into melts kept in contact with aluminium contained in a boron nitride crucible. A mass balance revealed that some gas was reduced to carbon.

Electrons may, to a certain degree, be transferred from the electrolyte phase to the anode,

$$e' = e^- \qquad (14)$$

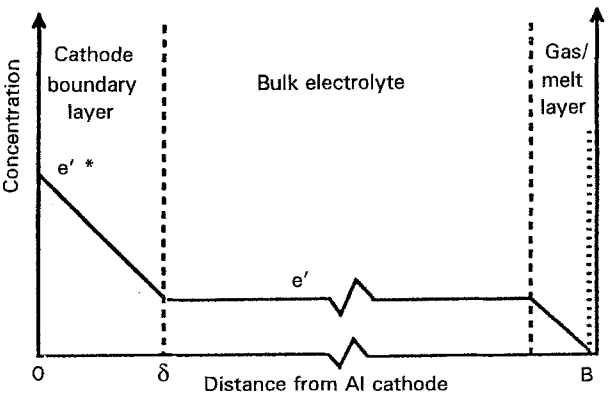

Fig. 2. Schematic concentration gradients of e′ (see text) in the boundary layers of an electrolyte free of impurities.

This direct transfer of electrons may be important at low current densities, when the rate of formation of anode gases is low.

2.3.2. Transport processes and reactions in the presence of impurities. The electrolytes in commercial cells always contain impurities which are introduced through alumina, anodes, tools etc. The presence of impurities probably alters the reaction/gradient scheme, because RE are expected to react readily with several of the impurities which can exist in more than one valence state in the electrolyte. Since the ionic structure of impurities dissolved in cryolitic melts are largely unknown, they are at present simply described in terms of uncomplexed ions. Johansen [31] found that iron contaminants in the electrolyte consisted of both Fe^{2+} and Fe^{3+} species (ratio $Fe^{2+}/Fe^{3+} \approx 70/30$). Commercial electrolytes usually contain several different impurity species, e.g. iron, phosphorus, silicon, vanadium, titanium and gallium [8]. Several attempts have been made to verify whether or not the bulk of electrolytes in commercial cells contain RE. Rolseth and Thonstad [32] treated bath samples with HCl and measured the amount of hydrogen gas evolved in order to determine bulk concentrations of reduced entities. A constant bulk concentration of RE corresponding to 0.01 wt % Al was found throughout the bulk of the electrolyte. It is probable, however, that hydrogen evolution may occur due to reaction between HCl and certain polyvalent impurities. Measurements of limiting currents may also be influenced by melt impurities, and may thus give erroneous results regarding bulk concentrations of RE in commercial cells. At present there is no conclusive experimental evidence as to whether or not the bulk phase in commercial cells contains RE.

It is, however, unlikely that RE should be transported past the impurities in the electrolyte bulk phase, not reacting with the impurities, but instead reacting with dissolved or gaseous carbon dioxide at the gas/electrolyte boundary layer. Polyvalent impurities of the highest oxidation state (such as Fe^{3+}) can probably not exist at measurable concentrations together with RE. The presence of RE should rapidly reduce the impurity species, if the reduced species, like Fe^{2+}, is soluble in the electrolyte.

In laboratory cells it has been observed that impurities can be reduced to a dispersed metallic state within the electrolyte phase after a certain time period in contact with liquid aluminium [33]. However, the mass transfer conditions in these laboratory cells can hardly reflect the conditions in commercial cells with continuous feeding of impurities.

In the following, the role of impurities in the process of metal loss is illustrated by considering iron impurities. From a thermodynamic and kinetic point of view it can be assumed that reactions of the type,

$$Fe^{3+} + e' = Fe^{2+} \qquad (15)$$

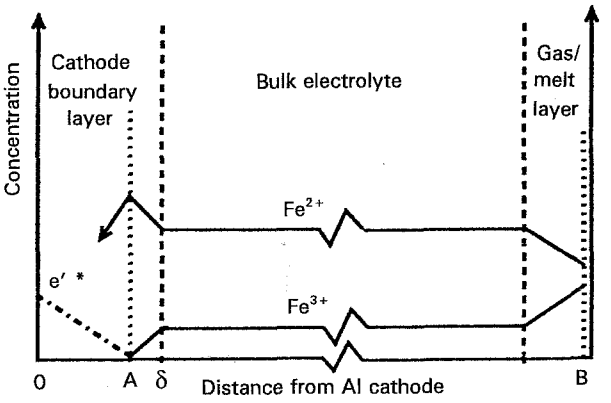

Fig. 3. Schematic concentration gradients of e′ (see text) and iron impurities in the cathode and the gas/melt boundary layers.

proceed rapidly to the right, which means that concentration gradients like the ones indicated in Fig. 3 are likely to develop. The fact that commercial cell electrolytes usually contain considerable amounts of impurities, suggests that Reaction 15 or similar ones with other impurities, probably take place in the cathodic boundary layer, as proposed by Sterten [5, 6]. The concentration of RE should then approach a very low equilibrium value in the reaction plane parallel to the metal surface and marked A in Fig. 3.

A fraction of the Fe^{2+} species formed according to Reaction 15 will diffuse towards the aluminium cathode and be reduced to Fe. The reduction site may be the aluminium surface itself. However, the reaction may also fully or partly take place in the electrolyte boundary layer, especially if nucleation sites like carbon dust and or alumina particles are present. Another fraction of the Fe^{2+} species formed by Reaction 15 will diffuse towards the bulk electrolyte phase.

The concentration of Fe^{3+} in the electrolyte is maintained both by 'fresh' impurities (from alumina feed etc.) and by the following equilibrium reaction with CO_2,

$$Fe^{2+} + 1/2CO_2 = Fe^{3+} + 1/2CO + 1/2O^{2-} \qquad (16)$$

Reaction 16 is most likely to occur in reaction plane B (Fig. 3) within the electrolyte/anode gas boundary layer (i.e., with CO and CO_2 dissolved in the cryolitic melt).

Finely dispersed carbon dust partly formed by Reaction 13 and partly by disintegration of the carbon anode will always be present, mostly in the upper part of the electrolyte in a commercial electrolysis cell. The Boudouard reaction,

$$CO_2(g) + C(s) = 2CO(g) \qquad (17)$$

will proceed somewhat to the right while gas bubbles are in direct contact with carbon particles. The bulk electrolyte concentrations of dissolved CO_2 are probably somewhat below saturation corresponding to the vapour pressure in the gas bubbles due to Reaction 16. It is not believed that Reaction 17 with dissolved CO_2 will be important in this context.

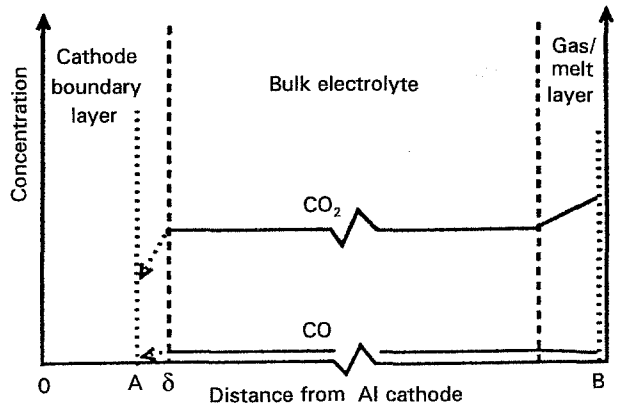

Fig. 4. Proposed concentration gradients of dissolved gas species in the boundary layers.

According to Bratland *et al.* [34] and Numata and Bockris [35] the solubility of CO_2 in cryolitic melts is in the order of 10^{-3}–10^{-2} mol dm^{-3} atm^{-1}. Numata and Bockris [35] found that the solubility of oxygen and inert gases was roughly 1/1000th of the solubility of CO_2. Unfortunately, there are no data available as to the solubility of CO in cryolite melts, but CO is expected to behave more like an inert gas, and to have a much lower solubility than CO_2, in analogy with behaviour of CO in other molten salts. If this assumption is correct, steady state concentration gradients of dissolved CO and CO_2, as shown in Fig. 4, may be expected with Reactions 10 and 13 probably taking place in the reaction plane A or on the metal surface.

The reaction plane A in Figs 3 and 4 is expected to move towards the metal phase with an increase of the electrolyte impurity level, giving rise to an increased flux of reduced entities from the cathode, and a subsequent decrease of CE. Considerable reductions of CE with small additions of various impurity species have been experienced by Szeker [36], Kerouanton and Badoz–Lambling [37], Gerlach and Deininger [38] and Anufrieva and Baranova [39].

An increase in cathode current density increases the NaF/AlF_3 ratio at the metal surface, giving rise to an increase in the equilibrium concentrations of RE at the cathode surface. The net result is (i) the production rate of Al increases due to increased fluxes of AlF_3 and NaF, and (ii) the rate of the loss process also increases due to increased fluxes of reduced species away from the metal surface. The reaction plane A moves towards the bulk electrolyte phase, but the corresponding change in CE is not easily predicted.

3. Summary of the reactions and transport steps: conclusions

The summary and conclusions presented below is based on the assumption that there are no, or only minor, concentration gradients in the bulk of the electrolyte phase, which requires a convective flow of the same order as usually present in commercial cells. The convective flow in laboratory cells during aluminium electrolysis may not fulfil this requirement.

The derivations below are also based on an impurity feed to the electrolyte in the same order of magnitude as in commercial aluminium electrolysis cells.

3.1. *Main cathode process*

The overall main cathode process at current densities of industrial importance may be separated in three steps:

(i) Mass transport of AlF_3 to the cathode (aluminium) interface.
(ii) The main overall electrode reaction, i.e., Equation 8,

$$AlF_3 + 3Na^+ + 3e^- = Al + 3NaF$$

(iii) Mass transport of NaF away from the cathode interface. (3 Na^+ is the charge transferred).

The rate limiting steps for this cathode process are the mass transport of AlF_3 and of NaF in the cathode boundary layer giving rise to a cathodic concentration overvoltage.

The main overall cell reaction consuming a charge of 3 F may be written,

$$1/2Al_2O_3 + 3/4C = Al + 3/4CO_2 \qquad (18)$$

3.2. *Reactions, mass transfer and rate limiting steps in the loss process*

The following steps are proposed for the loss process (see also Figs 3 and 4):

(i) Cathode side reactions (i.e., Equations 5, 6 and 7, repeated here for convenience) forming RE:

$$Na^+ + e^- = Na$$

$$1/2Na^+ + 1/2AlF_3 + e^- = 1/2AlF_2^- + 1/2NaF$$

$$e^- = e'$$

(ii) Corresponding main anode reaction (i.e., Equation 11),

$$1/2O^{2-} + 1/4C = 1/4CO_2 + e^-$$

(iii) Mass transport of RE from the cathode (metal) surface to the reaction plane A located in the cathodic diffusion layer, see Fig. 3.
(iv) Mass transport of reducible impurities from the electrolyte bulk phase towards the reaction plane A.
(v) Reactions between impurities and RE in plane A, exemplified by (Equation 15)

$$Fe^{3+} + e' = Fe^{2+}$$

(vi) Mass transport of reduced impurity species both towards the cathode where they are reduced to the metallic state, and towards the bulk of the electrolyte.
(vii) Convective mass transport of reduced impurity species through the bulk phase to the anode boundary layer.

(viii) Diffusive transport of reduced impurity species in the anode gas boundary layer to reaction site B, see Fig. 3.
(ix) Equilibrium reactions between impurities and dissolved anode gases in site B, for example, Equation 16,

$$Fe^{2+} + 1/2CO_2 = Fe^{3+} + 1/2CO + 1/2O^{2-}$$

(x) Mass transport of oxidized impurities (like Fe^{3+}) from site B towards the bulk electrolyte phase, where they will be involved in a new cycle, step (iv).

Combination of an arbitrary cathodic side reaction in step (i) with all other steps from (ii) to (x) gives the *overall loss process*, corresponding to a charge consumption of 1 F,

$$1/4CO_2 + 1/4C = 1/2CO \qquad (19)$$

The equation agrees with what can actually be observed; consumption of carbon and production of CO, at the expense of metal production. The amount of CO formed by the loss process is, of course, in agreement with the Pearson–Waddington formula [4] for CE with respect to aluminium. The above process is not a *chemical reaction* and should not be confused with the Boudouard Reaction 17, which is written in exactly the same way. The Boudouard reaction may contribute to an additional formation of CO, which may lead to an erroneous value of CE when based on analysis of gas composition and the Pearson–Waddington formula. Direct anodic oxidation of impurity species at the carbon anode surface may also take place to a certain degree, especially at low current densities, resulting in uncertainties in such CE calculations. However, it is important to note that at high current densities the *overall loss process* is formally the same regardless of whether the electrolyte phase is free from or contains minor amounts of impurities.

When considering the loss process, as for any chemical or electrochemical process, only rate determining steps are suitable for modelling. In commercial Hall–Heroult cells, with rapid convective mass transport in the electrolyte phase, the mass transport steps (iii) and (iv) in the cathode boundary layer are assumed to be the most important rate limiting steps in the loss process. The steps (iv), (vi), (viii) and (x) involving cyclic diffusion of impurities in the boundary layers will, of course, influence the flux of dissolved metal species away from the cathode, and as such be partly rate determining for the loss process. The rate limiting steps will be modelled in future work.

3.3. *Charge and material balance*

According to Equation 8, which can be considered as the reference equation, $3F$ is the charge needed to produce 1 mol of aluminium. Let CE $= x$ be the current efficiency ratio with respect to aluminium. The total charge transferred is then $3F/x$, while the difference in charge $((3F/x) - 3F)$ is consumed by the loss process, Equation 19. The loss process, rewritten as follows,

$$\frac{3}{4}\left(\frac{1}{x} - 1\right)CO_2 + \frac{3}{4}\left(\frac{1}{x} - 1\right)C = \frac{3}{2}\left(\frac{1}{x} - 1\right)CO \qquad (20)$$

describes the carbon and CO_2 consumption as a function of CE. Summation of Equation 18 and 20 describes on a molar basis the electrochemical material conversion equation,

$$\frac{1}{2}Al_2O_3 + \frac{3}{4x}C = Al + \frac{3}{4}\left(2 - \frac{1}{x}\right)CO_2 + \frac{3}{2}\left(\frac{1}{x} - 1\right)CO \qquad (21)$$

due to a total charge transfer of roughly $3F/x$.

When considering the heat or material balance of a commercial cell some other equations like the Boudouard reaction (17) should, of course, be included.

Acknowledgements

Financial support from The Research Council of Norway and from Norwegian aluminium industry is gratefully acknowledged. The work was performed in cooperation with Electrolysis Group, SINTEF Materials Technology.

References

[1] H. Ginsberg and H. C. Wrigge, *Metall.* **26** (1972) 997.
[2] N. Jarrett, in 'Production of Aluminium and Alumina', (edited by A. R. Burkin), John Wiley, New York (1987) chapter 13.
[3] H. Kvande, *Mag. Alum.* **26** (1989) 382.
[4] T. G. Pearson and J. Waddington, *Discuss. Faraday Soc.* **1** (1947) 307.
[5] Å. Sterten, *Acta Chem. Scand.* **44** (1990) 873.
[6] Å. Sterten, 'Light Metals', (edited by E. L. Rooy), Proceedings of the 120th TMS annual meeting (1991), p. 445.
[7] Å. Sterten, *J. Appl. Electrochem.* **18** (1988) 473.
[8] K. Grjotheim, C. Krohn, M. Malinovsky, K. Matiosovsky and J. Thonstad, 'Aluminium Electrolysis. Fundamentals of the Hall–Heroult process', 2nd ed., Aluminium-Verlag, Düsseldorf (1982).
[9] J. Thonstad, *Can. J. Chem.* **43** (1965) 3429.
[10] K. Yoshida and E. W. Dewing, *Met. Trans.* **3** (1972) 1817.
[11] R. Ødegård, Å. Sterten and J. Thonstad, *ibid.* **19B** (1988) 449.
[12] X. Wang, R. D. Peterson and N. Richards, Light Metals, (edited by E. L. Rooy), Proceedings of the 120th TMS annual meeting (1991), p. 323.
[13] E. W. Dewing and K. Yoshida, *Can. Met. Quart.* **15** (1976) 299.
[14] V. Borisoglebskii, M. M. Vetyukov and S. A. Nikiforov, *Sov. Electrochem.* **13** (1977) 506.
[15] R. Ødegård, 'Solubility and Electrochemical Behaviour of Al and Al_4C_3 in Cryolitic Melts', thesis, Norwegian Institute of Technology, Trondheim, Norway (1986).
[16] M. A. Bredig, 'Molten Salt Chemistry', (edited by M. Blander), Interscience Publishers, New York (1964), p. 367.
[17] J. J. Egan and W. Freyland, *Phys. Chem.* **89** (1985) 381.
[18] G. M. Haarberg, K. S. Osen, J. J. Egan, H. Heyer and W. Freyland, *Ber. Bunsenges. Phys. Chem.* **92** (1988) 139.
[19] J. Liu, J.-C. Poignet, *J. Appl. Electrochem.* **22** (1992) 1110.
[20] G. M. Haarberg, K. S. Osen, J. Thonstad, R. J. Heus and J. J. Egan, *ibid.* **137** (1990) 2777.
[21] E. W. Dewing, *Met. Trans.* **22B** (1991) 669.

[22] R. Piontelli, G. Montanelli and G. Sternheim, *Rev. Metall.* **53** (1956) 248.
[23] R. Piontelli, *Electrochim. Metall* **1** (1966) 191.
[24] J. Thonstad and S. Rolseth, *Electrochim. Acta* **23** (1978) 221.
[25] *Idem, ibid.* **23** (1978) 233.
[26] E. Sum and M. Skyllas-Kazacos, *ibid.* **23** (1978) 677.
[27] W. B. Frank and L. M. Foster, *J. Phys. Chem.* **61** (1957) 1531.
[28] S. K. Ratkje, H. Rajabu and T. Førland, *Electrochim. Acta* **37** (1992) 415.
[29] Å. Sterten, *ibid.* **25** (1980) 1673.
[30] J. Thonstad, *J. Electrochem. Soc.* **111** (1964) 955.
[31] H. G. Johansen, 'Jern som forurensningselement i aluminium elektrolysen', thesis, Department of Electrochemistry, Norwegian Institute of Technology, Trondheim, Norway (1975).
[32] S. Rolseth and J. Thonstad, Light Metals, (edited by G. M. Bell), Proceedings of the 110th TMS annual meeting (1981), p. 289.
[33] P. Chin, 'The Behaviour of Impurity Species in Hall–Heroult Aluminium Cells', Dissertation, Carnegie Mellon University, Pittsburgh, Pennsylvania (1992).
[34] D. Bratland, K. Grjotheim, C. Krohn and K. Motzfeldt, *J. Metals* **19** (1967) 13.
[35] H. Numata and J. O'M. Bockris, *Met. Trans.* **15B** (1984) 39.
[36] C. Szeker, *Acta Technika Acad. Sci. Hung.* **10** (1954) 19.
[37] A. Kerouanton and J. Badoz-Lambling, *Rev. Chim. Minerale* **11** (1974) 223.
[38] J. Gerlach and L. Deininger, *Metall* **33** (1979) 31.
[39] N. I. Anufrieva, L. S. Baranova and Z. N. Balashova, *Sov. J. Non-Ferrous Met.* **24** (1983) 38.